

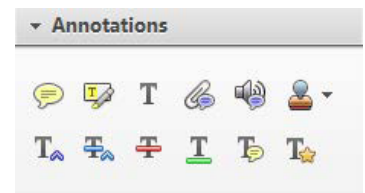
## Smart Proof System Instructions

It is recommended that you read all instructions below; even if you are familiar with online review practices.

Using the Smart Proof system, proof reviewers can easily review the PDF proof, annotate corrections, respond to queries directly from the locally saved PDF proof, all of which are automatically submitted directly to **our database** without having to upload the annotated PDF.

- ✓ **Login into Smart Proof** anywhere you are connected to the internet.
- ✓ **Review the proof** on the following pages and mark corrections, changes, and query responses using the **Annotation Tools**.

**Note:** Editing done by replacing the text on this PDF is not permitted with this application.



- ✓ **Save your proof corrections** by clicking the "Publish Comments" button.  
Corrections don't have to be marked in one sitting. You can publish comments and log back in at a later time to add and publish more comments before you click the "Complete Proof Review" button below.
- ✓ **Complete your review** after all corrections have been published to the server by clicking the "Complete Proof Review" button below.

### **Before completing your review.....**

Did you reply to all author queries found in your proof?

Did you click the "Publish Comments" button to save all your corrections?  
Any unpublished comments will be lost.


**Note:** Once you click "Complete Proof Review" you will not be able to add or publish additional corrections.

## Adding Comments and Notes to Your PDF

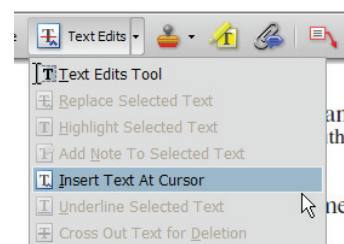
**IMPORTANT:** Composition cannot be completed until the author review is complete and all changes and author query answers have been added to this proof. Author queries are found at the end of this pdf.

To facilitate electronic transmittal of corrections, we encourage authors to utilize the comments and notes features in Adobe Acrobat. The PDF provided has been “comment-enabled,” which allows you to utilize the comments and notes features, even if using only the free Adobe Acrobat reader (see note below regarding acceptable versions). Adobe Acrobat’s Help menu provides additional details on the tool. When you open your PDF, the comments/notes/edit tools are clearly shown on the tool bar (though icons may differ slightly among versions from what is shown below).

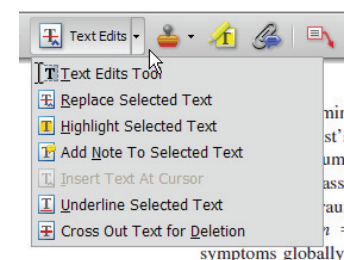
For purposes of correcting the PDF proof of your journal article, the important features to know are the following:


- Use the **Text Edits tool**,  Text Edits, to insert, replace, or delete text.

- To **insert text**, place your cursor at a point in text and select “Insert Text at Cursor” from the text edits menu. Type your additional text in the pop-up box.



- To **replace text** (do this instead of deleting and then re-inserting), highlight the text to be changed, select “Replace Selected Text” from the text edits menu, and type the new text in the pop-up box.



- To **delete text**, highlight the text to be deleted and select “Cross Out Text for Deletion” from the text edits menu (see graphic above).
- Use the **Sticky Note tool**,  Sticky Note, to describe changes that need to be made (e.g., changes in bold, italics, or capitalization use; altering or replacing a figure) or to answer a question or approve a change that was posed by the editor. To use this feature, click on the sticky note tool and then click on a point in the PDF where you would like to make a comment, then type your comment in the pop-up box.



- Use the **Callout tool**, , to point directly to changes that need to be made. Try to put the callout box in an area of white space so that you do not obscure the text, as in the example below.

Table 5

*Experiment 4: Comparative Optimism as a Function of Self-Presentation and Event Valence*

Self-presentation	Event					
	Positive		Negative		Total	
	<i>M</i>	<i>SD</i>	<i>M</i>	<i>SD</i>	<i>M</i>	<i>SD</i>
Public/student	3.46	0.13	3.60	0.10	3.53	0.12
Public/expert	2.66	0.12	2.78	0.13	2.73	0.13
Control	2.39	0.11	2.46	0.09	2.43	0.11
Total	2.84	0.47	2.95	0.50		

The first column's entries should be flush left (except for "Total", which should be indented one em-space), as in Tables 1 and 2 previously.

- Use the **Highlight tool**, , to indicate font problems, bad breaks, and other textual inconsistencies. Describe the inconsistencies with the callout tool (shown) or a sticky note. One callout (or sticky note) can describe many changes.

$$du/dt = -\lambda v^\alpha = -\lambda u$$

$$du/u = -\lambda dt$$

$$u_t = ue^{-\lambda t}.$$

Close up minus sign to lambda (3 times, highlighted)

An alternate method is to select the appropriate text with your cursor, select **"Add Note to Selected Text"** from the text edits menu, and then type your note in the pop-up box (the selected text is highlighted automatically).

As with hand-annotated proof corrections, the important points are to communicate changes clearly and thoroughly; to answer all queries and questions; and to provide complete information for us to make the necessary changes to your article so it is ready for publication.

To utilize the comments/notes features on this PDF you will need Adobe Reader version 7 or higher. This program is freely available and can be downloaded from <http://get.adobe.com/reader/>



# A Ribosomal Protein Homolog Governs Gene Expression and Virulence in a Bacterial Pathogen

AQ: au Hannah S. Trautmann,<sup>a</sup> Kathryn M. Ramsey<sup>a,b</sup>

<sup>a</sup>Department of Cell and Molecular Biology, University of Rhode Island, Kingston, Rhode Island, USA

<sup>b</sup>Department of Biomedical and Pharmaceutical Sciences, University of Rhode Island, Kingston, Rhode Island, USA

**ABSTRACT** The molecular machine necessary for protein synthesis, the ribosome, is generally considered constitutively functioning and lacking any inherent regulatory capacity. Yet ribosomes are commonly heterogeneous in composition and the impact of ribosome heterogeneity on translation is not well understood. Here, we determined that changes in ribosome protein composition governed gene expression in the intracellular bacterial pathogen *Francisella tularensis*. *F. tularensis* encoded three distinct homologs for bS21, a ribosomal protein involved in translation initiation, and analysis of purified *F. tularensis* ribosomes revealed they were heterogeneous with respect to bS21. The loss of one homolog, bS21-2, resulted in significant changes to the cellular proteome unlinked to changes in the transcriptome. Among the reduced proteins were components of the type VI secretion system (T6SS), an essential virulence factor encoded by the *Francisella* pathogenicity island. Furthermore, loss of bS21-2 led to an intramacrophage growth defect. Although multiple bS21 homologs complemented the loss of bS21-2 with respect to T6SS protein abundance, bS21-2 was uniquely necessary for robust intramacrophage growth, suggesting bS21-2 modulated additional virulence gene(s) distinct from the T6SS. Our results indicated that ribosome composition in *F. tularensis*, either directly or indirectly, posttranscriptionally modulated gene expression and virulence. Our findings were consistent with a model in which bS21 homologs function as posttranscriptional regulators, allowing preferential translation of specific subsets of mRNAs, likely at the stage of translation initiation. This work also raised the possibility that bS21 in other organisms may function similarly and that ribosome heterogeneity may permit many bacteria to posttranscriptionally regulate gene expression.

**IMPORTANCE** While bacterial ribosomes are commonly heterogeneous in composition (e.g., incorporating different homologs for a ribosomal protein), how heterogeneity impacts translation is unclear. We found that the intracellular human pathogen *Francisella tularensis* had heterogeneous ribosomes, incorporating one of three homologs for ribosomal protein bS21. Furthermore, one bS21 homolog posttranscriptionally governed the expression of the *F. tularensis* type VI secretion system, an essential virulence factor. This bS21 homolog was also uniquely important for robust intracellular growth. Our data supported a model in which bS21 heterogeneity led to modulation of translation, providing another source of posttranscriptional gene regulation. Regulation of translation by bS21, or other sources of ribosomal heterogeneity, may be a conserved mechanism to control gene expression across bacterial phylogeny.

**KEYWORDS** *Francisella*, gene regulation, posttranscriptional control mechanisms, ribosomal proteins, virulence regulation

Regulation of translation provides bacteria with a rapid way to modify gene expression. While many distinct mechanisms permit this fine-tuning (1, 2) the impact of ribosome composition on gene expression remains poorly understood. In bacteria, ribosomes are diverse and commonly heterogeneous with respect to ribosomal protein (r-protein)

**Editor** Patricia A. Champion, University of Notre Dame

**Copyright** © 2022 Trautmann and Ramsey. This is an open-access article distributed under the terms of the [Creative Commons Attribution 4.0 International license](#).

Address correspondence to Kathryn M. Ramsey, [kramsey@uri.edu](mailto:kramsey@uri.edu).

The authors declare no conflict of interest.

**Received** 14 July 2022

**Accepted** 24 August 2022

content, posttranslational modifications, rRNA content, or posttranscriptional modifications (reviewed in reference (3)). The functional consequences of ribosome heterogeneity are unclear but may include the formation of “specialized ribosomes,” or ribosomes with altered activity due to their distinct composition (4). Although specialized ribosomes are not well described in bacteria, exciting recent studies have connected altered rRNA content of ribosomes and gene regulation (5, 6) and, in *Mycobacterium smegmatis*, ribosomes containing alternate r-protein homologs translate some genes with differential efficiency (7).

*Francisella tularensis* is a Gram-negative, facultative intracellular bacterium that causes the potentially fatal human disease tularemia (8). After internalization into host cells, *F. tularensis* must escape from the Francisella-containing phagosome to replicate inside the cytosol. This escape process requires a type VI secretion system (T6SS), which modifies the host cell by delivery of effector proteins (9–12). Production of this T6SS is coordinately regulated by the transcription factors MglA, SspA, and PigR, as well as the signaling molecule ppGpp (13–20). Regulation of the T6SS is arguably the most well-understood virulence regulatory network in *F. tularensis*. However, much remains to be learned about the regulation of other virulence factors.

Despite its relatively small genome (<2 Mbp), *F. tularensis* encodes three distinct *rpsU* genes (*rpsU1*, *rpsU2*, and *rpsU3*), which encode homologs of the small ribosomal subunit protein bS21 (bS21-1, bS21-2, and bS21-3, respectively). This is the only apparent source of ribosome heterogeneity in *F. tularensis*, as the three rRNA operon sequences are identical and no other r-proteins are encoded by multiple homologs. In *Escherichia coli*, bS21 is involved in translation initiation (21, 22) and, consistent with this activity, is found on the ribosome close to the anti-Shine-Dalgarno sequence near the mRNA exit channel (23, 24). Furthermore, bS21 is one of the last r-proteins to assemble into the ribosome, is considered “loosely associated,” and is easily exchanged among assembled ribosomes (25, 26).

Using mass spectrometry and immunoblot analyses, we showed that ribosomes in *F. tularensis* were heterogeneous with respect to bS21 content and could incorporate any of the three bS21 homologs into actively translating ribosomes. Using quantitative whole-cell proteomics, quantitative immunoblots, and transcriptomic analyses, we demonstrated that loss of a particular bS21 homolog, bS21-2, led to changes in abundance for a subset of proteins that could not be explained by changes in transcript abundance. Among the impacted proteins were multiple virulence factors, including those that comprise the T6SS. Finally, using intramacrophage growth assays, we provided evidence that bS21-2, and not the other bS21 homologs, promoted intramacrophage growth. Our findings revealed that a specific r-protein homolog in *F. tularensis*, bS21-2, governed gene expression at the level of protein abundance and positively impacts virulence.

## RESULTS

**Francisella species encoded three bS21 homologs.** The genomes of multiple Francisella species contain three distinct genes encoding bS21 (*rpsU1*, *rpsU2*, and *rpsU3*), raising the possibility that cells contain ribosomes that were heterogeneous with respect to bS21 content. The gene encoding one homolog in *F. tularensis*, *rpsU2* (encoding bS21-2), was syntenic with the single bS21-encoding gene in *Escherichia coli* (Fig. S1 in Supplemental File 1). In *E. coli*, *rpsU* was the first in an operon referred to as the macromolecular synthesis operon, encoding key proteins for initiation of translation (bS21), DNA replication (DNA primase), and transcription (RNA polymerase  $\sigma^{70}$ ) (27). The corresponding operon in Francisella species, including *F. tularensis*, also contains *yqeY*, which may encode a protein necessary for correct tRNA aminoacylation (28). Another bS21 homolog, bS21-1, was encoded by *rpsU1* in an apparent operon downstream of the gene for cold shock protein CspC. There were no annotated genes in the same transcriptional context as *rpsU3*, the gene encoding the third homolog, bS21-3. The bS21 homologs in *F. tularensis* were distinct but similar, with amino acid identities ranging from 48 to 72%, and were similar to *E. coli* bS21 (51 to 60% identical, with bS21-2 having the highest identity; Fig. S2 in Supplemental File 1).

AQ: B



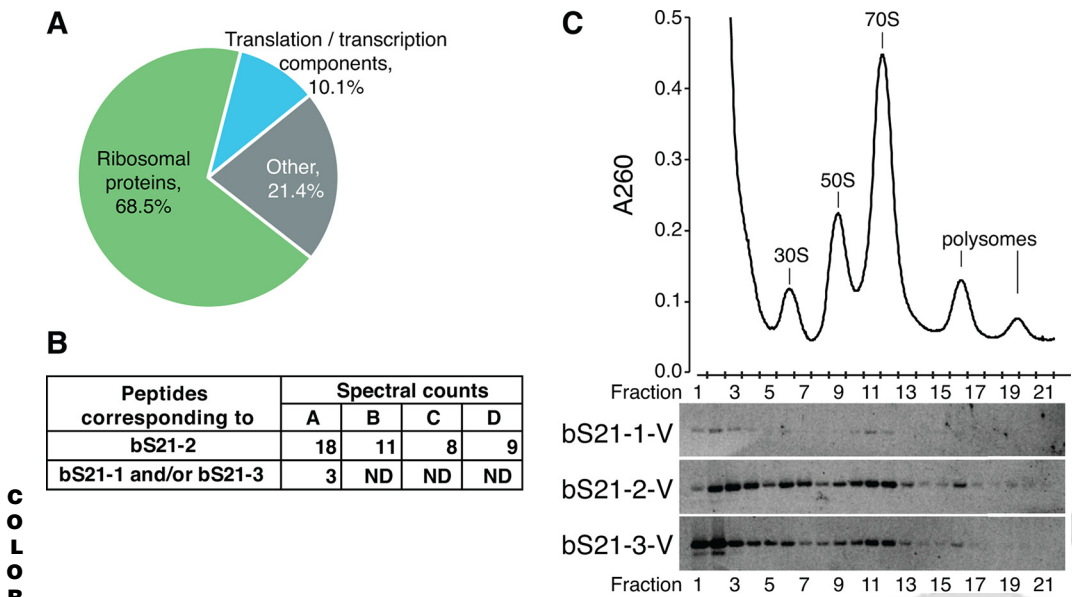


**FIG 1** *F. tularensis* ribosomes were heterogeneous with respect to bS21. (A) A chart demonstrating the purity of wild-type ribosomes. Categories represent the classification of proteins identified by mass spectrometry of ribosomes purified from wild-type *F. tularensis* LVS cells. Numbers represent the percentage of spectral counts corresponding to proteins in each category, combined from quadruplicate samples. (B) Wild-type *F. tularensis* LVS ribosomes contain more than one bS21 homolog. A table detailing the number of spectral counts corresponding to bS21 homologs identified from individual ribosome purifications (A to D) from wild-type cells. Spectral counts corresponding to bS21-1 and/or bS21-3 could not be unambiguously assigned due to the complete sequence identity of detected peptides. ND: not detected. (C) Each bS21 homolog could be incorporated into ribosomes. Top, sucrose gradient sedimentation profile from actively translating wild-type cells containing an empty vector. Nucleic acid content was monitored by the absorbance at 260 nm ( $A_{260}$ ) (y-axis). Peaks corresponding to the 30S, 50S, 70S, and polysomes are indicated. Fractions collected are indicated on the x-axis. Bottom, immunoblot analysis of fractions from sucrose gradient sedimentation performed on actively translating cells ectopically expressing indicated bS21 homolog with VSV-G epitope tag. Wells correspond to fractions 1 to 21 from the profile above.

***F. tularensis* ribosomes were heterogeneous.** The presence of three distinct genes encoding bS21 raises the potential for *F. tularensis* ribosomes to be heterogenous with respect to bS21. To investigate this possibility, we used sucrose cushion centrifugation to isolate ribosomes from *F. tularensis* LVS grown *in vitro* in quadruplicate and analyzed their protein composition using liquid chromatography-tandem mass spectrometry (LC-MS/MS). Approximately 80% of the spectral counts corresponded to ribosomal proteins or proteins associated with transcription and translation complexes (e.g., RNA polymerase, translation release factors, SRP), indicating *F. tularensis* ribosomes purified in this manner were highly pure (Fig. 1A, Table S1 in Supplemental File 2). Despite the small size of bS21 (approximately 8 kDa), we identified multiple peptides corresponding to bS21-2 in all samples. In one sample, peptides shared between bS21-1 and bS21-3 were detected (Fig. 1B). This suggested that bS21-2 was the most abundant homolog in wild-type cells, consistent with its production from operon encoding proteins essential for transcription and DNA replication. It also suggested that either bS21-1, bS21-3, or both, were incorporated into ribosomes in LVS. However, it did not allow us to determine the next-most abundant homolog (bS21-1 or bS21-3) or confirm the incorporation of both other homologs. Regardless, these results demonstrated that multiple bS21 homologs were incorporated into wild-type *F. tularensis* ribosomes and that ribosomes in *F. tularensis* were heterogenous, containing different bS21 homologs.

We next wanted to determine if each bS21 homolog could be found in actively translating ribosomes. To track each bS21, we modified each homolog to encode a C-terminal vesicular stomatitis virus glycoprotein (VSV-G) tag and individually ectopically expressed them, using the same promoter, from a plasmid in wild-type cells. Lysate fractions of these cells were analyzed by immunoblotting after sucrose gradient sedimentation (Fig. 1C; Fig. S3 in Supplemental File 1). When ectopically expressed (rather

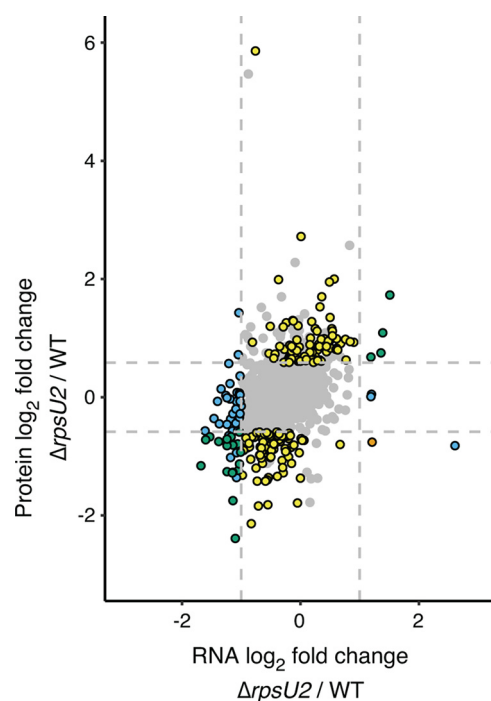


**FIG 2** Loss of bS21-2 led to changes in protein abundance that could not be explained by changes in transcript abundance. Cells with (WT, wild-type) and without bS21-2 ( $\Delta rpsU2$ ) were analyzed using RNA-seq (x-axis) and DIA whole-cell mass spectrometry (y-axis). Genes are represented by dots. Most genes with changes in protein (161 yellow dots) did not have corresponding changes in transcript abundance. One gene (orange dot) had discordant changes in transcript and protein abundance. Green dots (23) represent genes with concordant changes in transcript and protein abundance. Blue dots (60) indicate genes with altered transcript abundance only. Horizontal dashed lines indicate a  $\pm 1.5$ -fold cutoff for differential protein abundance; vertical dashes indicate a  $\pm 2$ -fold cutoff for differential transcript abundance. Colored dots with black outlines represent genes with significant changes in protein ( $\pm 1.5$ -fold change, adjusted  $P < 0.05$ ) and/or transcript ( $\pm 2$ -fold change, adjusted  $P < 0.05$ ) abundance as indicated above, while gray dots without outline represent genes with changes that did not meet the statistical thresholds. Three gray dots are located outside the bounds of the axis as represented.

than produced from its native locus), bS21-1 was the least abundant homolog while bS21-3 was produced at the highest level. Each homolog was found in fractions corresponding to the 30S, 70S, and polysomes. Although bS21 was thought to function primarily in translation initiation, our findings indicated that each bS21 homolog was associated with the ribosome throughout the translation cycle.

**Loss of bS21-2 led to changes in protein, but not transcript, abundance.** Because the ribosomal protein bS21 was involved in translation initiation, we hypothesized that loss of a bS21 homolog may impact translation and result in changes in abundance in a subset of proteins. To test this hypothesis, we individually deleted each of the three genes encoding bS21 homologs. This led us to determine that no single bS21 homolog was essential for cell growth. We subsequently grew wild-type cells and cells lacking single bS21 homologs to the mid-log phase *in vitro* and used data-independent acquisition (DIA) mass spectrometry analysis (29) to compare relative protein abundance in cell lysates. Using this method, 68% of the total proteins predicted to be encoded by *F. tularensis* LVS were identified and analyzed (1194 of 1754). Compared to wild-type, we did not detect any significant changes in protein abundance in cells lacking either of the two lower-abundance bS21 homologs, bS21-1 and bS21-3 ( $>1.5$ -fold altered with an adjusted  $P < 0.05$ , excluding bS21). In contrast, cells lacking the most abundant homolog, bS21-2 ( $\Delta rpsU2$ ), had significant proteomic differences compared to wild-type cells. Specifically, we found 185 unique proteins ( $\sim 16\%$  of detected proteins) had altered abundance in cells without bS21-2 compared to wild-type cells (Fig. 2, data on the y-axis; Table S2 in Supplemental File 3).

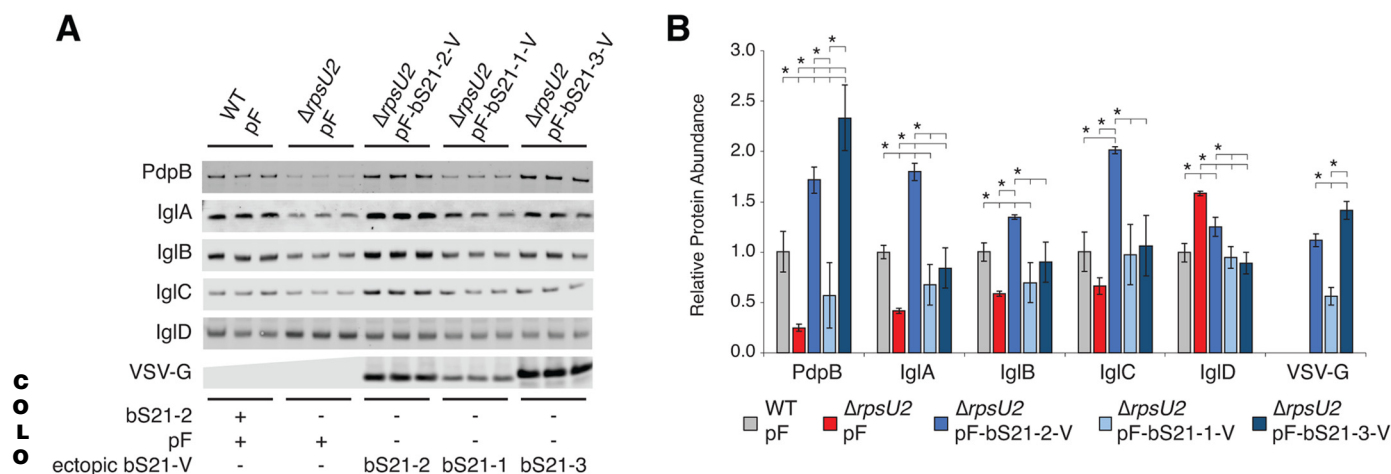


**FIG 3** bS21-2 impacted T6SS protein abundance. (A) Immunoblot analysis of indicated T6SS protein abundance. Cells either contained (wild-type) or lacked ( $\Delta rpsU2$ ) bS21-2 and either an empty vector control (pF) or a vector ectopically expressing VSV-G-tagged bS21 homologs (pF-bS21-1-V, pF-bS21-2-V, or pF-bS21-3-V). Immunoblot against VSV-G was included to demonstrate the production of VSV-G-tagged bS21 homologs. (B) Quantification of immunoblots from (A). Band intensities for each protein were normalized to total protein per well on the membrane. Error bars represent 1 SD. Experiments were repeated at least twice and data from a representative experiment are shown. The lines above bars indicate statistical comparison among groups by *t* test. Asterisk indicates the group to which all other groups are compared if the horizontal line connects to the line above group; \*, *P* < 0.05 using Benjamini-Hochberg correction.

To determine if these changes in protein abundance could be explained by corresponding changes in transcription, we performed transcriptomic analyses on wild-type cells, cells lacking bS21-2 ( $\Delta rpsU2$ ), and cells lacking the native bS21-2 but ectopically expressing bS21-2-V from a plasmid. Comparing cells with and without native bS21-2, we identified 105 differentially expressed genes (>2-fold altered with an adjusted *P* < 0.05, excluding *rpsU*; Fig. 2, data on the x-axis, Table S3 in Supplemental File 4). All these changes were complemented by ectopic expression of bS21-2-V on a plasmid.

Our analysis revealed that in cells lacking bS21-2, the largest change in transcript abundance was a 6-fold increase in *yqeY*, the gene directly downstream from *rpsU2*, which encoded bS21-2. This increase in transcript abundance was complemented by the ectopic expression of bS21-2-V, suggesting that bS21-2 functioned as a negative regulator of its operon. Translational feedback regulation was well-established for multiple ribosomal proteins (30, 31), but, to the best of our knowledge, this was the first report of translational regulation of ribosomal proteins in *F. tularensis* and that bS21 governed its production.

A comparison of our proteomic and transcriptomic analyses revealed that the changes in protein abundance were not generally due to changes in transcript abundance. Of the 185 differentially abundant proteins in cells lacking bS21-2, only ~12% (23) could be explained by altered transcription (Fig. 2, yellow dots), while about 88% (162; Fig. 2, blue dots and orange dot) had changes in protein abundance without a corresponding change in transcript abundance. These discrepancies between transcript abundance and protein abundance support a model in which bS21-2 controls the expression, either directly or indirectly, of some genes at the level of translation.

**bS21-2 governed the abundance of type VI secretion system proteins, which were essential for virulence.** Among the proteins with altered abundance in cells lacking bS21-2, we identified 12 out of 16 proteins encoded on the *Francisella* pathogenicity island (FPI). The FPI encodes a unique type VI secretion system (T6SS) that is essential for intramacrophage growth and virulence of *F. tularensis* (32–34). Using quantitative immunoblotting and antibodies specific to a subset of *F. tularensis* T6SS proteins, we validated that cells lacking bS21-2 have differences in those T6SS proteins (Fig. 3). Consistent with the mass spectrometry results, we found reductions in virtually all probed T6SS proteins, including an ~4-fold reduction in PdpB, the TssM/IcmF homolog. Using this approach, we also found an ~2.4-fold reduction in IglA and ~1.7-fold reduction in IglB, and T6SS proteins that were just below the cutoff for statistical significance in our mass spectrometry analysis. Because



we identified this differential abundance using a more sensitive method of comparison, it raised the possibility that all FPI-encoded proteins may be differentially abundant in cells lacking bS21-2 compared to wild-type cells, but we did not have antibodies specific to the remaining proteins (i.e., PdpE and VgrG) to test this hypothesis. Also consistent with our mass spectrometry findings, IgID (the homolog of TssK) was the only T6SS protein with increased, rather than decreased, protein abundance (Fig. 3). Each of these changes in protein abundance could be complemented by ectopic expression of bS21-2-V, driven by the *groES* promoter on a plasmid (Fig. 3).

These changes in protein abundance likely reflect positive regulation of most, but not all, T6SS proteins by bS21-2 at the level of translation, either directly or indirectly. Our findings were inconsistent with bS21 positively regulating transcription. It is well-established that transcription of FPI operons is coordinately controlled, and our RNA-seq analysis revealed that cells lacking bS21-2 did not have FPI-wide transcript reductions (13–16, 20, 35) (Table S3 in Supplemental File 4). In a complementary approach, we compared the transcript abundance for specific FPI genes using quantitative RT-PCR and included cells lacking PigR, a transcription factor critical for positive transcriptional regulation of FPI genes (14–16, 20, 35) (Fig. S4 in Supplemental File 1). We confirmed that cells lacking PigR have major decreases in FPI transcript abundance, but cells lacking bS21-2 did not have compelling (2-fold or greater) changes in FPI transcript abundance or transcript abundance of the positive regulator PigR, consistent with the RNA-Seq results. We considered the possibility that loss of bS21-2 could indirectly impact T6SS protein abundance by altering protein stability, but the half-life of one of the most differentially abundant proteins, PdpB, was unchanged in cells with and without bS21-2 (longer than 120 min, Fig. S5 in Supplemental File 1). Our results were consistent with bS21-2 controlling the expression of T6SS proteins at the level of translation.

**Other bS21 homologs impacted the abundance of type VI secretion system proteins.** Our findings indicated that bS21-2 was the most abundant bS21 homolog in wild-type cells. However, it was not clear if most ribosomes in cells lacking bS21-2 incorporate another bS21 homolog or no bS21 at all. This led to the question: did all bS21 homologs affect T6SS protein translation or did bS21-2 specifically modulate the translation of T6SS proteins? To answer this question, we ectopically expressed either bS21-1-V or bS21-3-V in cells lacking bS21-2, similarly to the ectopic expression of bS21-2-V. We subsequently used quantitative immunoblot analyses to assess the abundance of each ectopically expressed bS21 homolog and a subset of T6SS proteins (Fig. 3). While this strategy resulted in comparable amounts of bS21-2 and bS21-3, ectopic expression resulted in approximately 2-fold less bS21-1 than the other homologs, consistent with its lower expression in wild-type cells (Fig. 1 and 3). With respect to T6SS protein abundance, ectopic expression of bS21-3 restored all probed proteins to wild-type levels, complementing the loss of bS21-2 (Fig. 3). However, bS21-1 did not appear to complement T6SS protein production completely (Fig. 3). This may be due to reduced levels of bS21-1, lack of specific ability to regulate T6SS proteins, or a combination of the two factors. Notably, loss of bS21-2 resulted in a growth defect (Table S4 in Supplemental File 5) that could be complemented by ectopic expression of bS21-2 or bS21-1, but not bS21-3. The fact that cells lacking bS21-2 with ectopic expression of bS21-3 had wild-type levels of T6SS proteins and yet still had a growth defect revealed that changes in T6SS proteins were not due simply to changes in growth rate. Our findings allowed us to conclude that incorporation of either bS21-2 or bS21-3 – and to a lesser extent, bS21-1 – into ribosomes modulated the production of T6SS proteins.

**bS21-2 was important for intramacrophage growth.** A functional T6SS is essential for *F. tularensis* intramacrophage replication and is a strict requirement for virulence (32–34). The observed differences in FPI protein abundance led us to hypothesize that T6SS function may be compromised in cells lacking bS21-2 and these cells may be attenuated for intramacrophage growth. We tested the ability of cells lacking bS21-2 ( $\Delta rpsU2$ ) to survive in murine macrophage-like J774A.1 cells. This revealed a significant defect in the ability of bS21-2 mutant cells to replicate in macrophages. We recovered 10-fold fewer bS21-2 mutant bacteria after 24 h compared to wild-type (Fig. 4). The

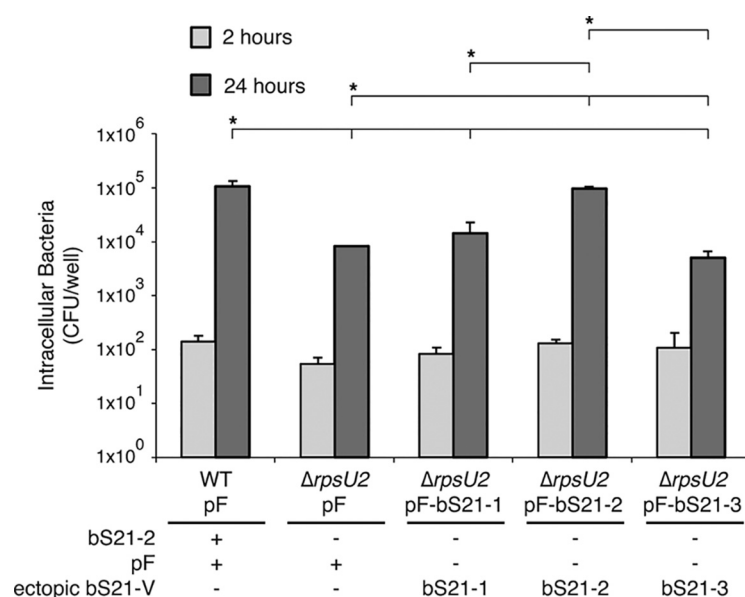


**FIG 4** Cells without bS21-2 had an intramacrophage growth defect, which could be complemented by the ectopic expression of bS21-2. Growth and survival of *F. tularensis* LVS cells within J774A.1 cell. Murine macrophage-like J774A.1 cells were infected with indicated bacterial cells at a multiplicity of infection of 5 to 10. J774A.1 cells were lysed, and bacteria were plated for enumeration (CFU) at 2 h and 24 h postinfection. Error bars represent 1 SD. Experiments were repeated at least twice and data from a representative experiment are shown. The lines above bars indicate statistical comparison among groups by *t* test. An asterisk indicates the group to which all other groups were compared if the horizontal line connects to the line above the group; \*,  $P < 0.05$  using Benjamini-Hochberg correction.

intramacrophage growth defect of cells lacking bS21-2 could be restored by ectopic expression of bS21-2 from a plasmid (Fig. 4). This contrasted with the ectopic expression of bS21-1 and bS21-3, neither of which restored the intramacrophage growth of cells lacking bS21-2 (Fig. 4). These results indicated that bS21-2 was specifically required for intramacrophage survival, even though the ectopic expression of bS21-1 restored *in vitro* growth rates and ectopic expression of bS21-3 restored T6SS protein production *in vitro* (Fig. 3; Table S4 in Supplemental File 5).

In summary, only the presence of bS21-2, not bS21-1 or bS21-3, could restore the intramacrophage growth defect of cells without bS21-2. This revealed that bS21-2 was critical for *F. tularensis* virulence and fits a model in which bS21-2 specifically regulated one or more genes necessary for intramacrophage growth in addition to T6SS genes, a topic still under investigation.

## DISCUSSION

The findings described here revealed that ribosome composition in *F. tularensis* was heterogeneous with respect to the small ribosomal protein bS21 and that this heterogeneity impacted gene expression at the level of translation. By studying cells that contain ribosomes either with or without one of the three bS21 homologs, we identified that bS21-2 governed the abundance of most T6SS proteins. Additionally, cells lacking bS21-2 were defective for intramacrophage growth. Because this intramacrophage growth defect could only be complemented by bS21-2, even though bS21-3 and (to a lesser extent) bS21-1 could restore T6SS protein abundance, it likely independent of the impact bS21-2 has on the T6SS. This allowed us to conclude that bS21-2 was important for intramacrophage growth of *F. tularensis*, potentially by regulating the translation of one or more proteins (in addition to the T6SS) necessary for virulence.

To examine the impact of bS21 homologs on gene expression, we used tools that assess the steady-state abundance of protein and transcripts: mass spectrometry and RNA-seq, respectively. Our analyses revealed that compared to wild-type cells, cells

lacking bS21-2 have changes in protein abundance that could not be explained by steady-state changes in corresponding mRNAs. Yet for some proteins with altered abundance in cells lacking bS21-2, there were corresponding modest differences in transcript abundance that did not reach statistical significance (Fig. 2, yellow dots). Loss of bS21-2 may lead to modest transcript abundance changes that result in more significant changes in protein abundance. But given the role of bS21 in translation, and specifically translation initiation, we proposed a model in which bS21-2 impacted gene expression by modulating translation initiation for specific mRNAs. Because an mRNA can be stabilized by translation, increased translation can increase stability and, conversely less translation can lead to faster degradation (reviewed in reference (36)). This effect may impact the abundance of many transcripts in cells lacking bS21-2 and may explain the observed weak correlation between some protein and transcript abundances. Consequently, additional work will be required to validate our model.

Our approach to studying bS21 homologs in *F. tularensis* has thus far focused on the homolog bS21-2, whose loss led to phenotypic changes. Our data suggested that bS21-2 was the most abundant homolog under the conditions studied. We hypothesized that cells without bS21-1 and bS21-3 did not exhibit distinct phenotypes under the conditions of our experiments due to their relatively low abundance. Both homologs may also influence gene expression under conditions when they were more abundant, but these conditions were not yet identified. Additionally, in our study of cells without bS21-2, it was not clear if most ribosomes lack bS21 entirely or instead incorporated bS21-1 or bS21-3. Our findings only extend to heterogeneity with respect to the presence or absence of bS21-2.

A comparison of *rpsU* genes across the bacterial phylogeny revealed that many clades and species did not encode bS21, suggesting that it was not essential for translation (37, 38). However, targeted deletion of the single *rpsU* gene in *E. coli* has not been successful, suggesting bS21 is essential in *E. coli* (39–41). We reported in previous work that the *F. tularensis* homolog syntenic with *E. coli rpsU*, *rpsU2*, is essential *in vitro* using transposon-insertion sequencing (Tn-Seq) (42). Yet using a targeted allelic exchange approach, we have been able to successfully delete each *rpsU* homolog individually, indicating that none of the *F. tularensis* bS21 homologs is individually essential. Our identification of *rpsU2* as an essential gene was likely due to the polar effects of transposon insertion into the first gene of an operon containing other known essential genes (*dnaG*, encoding primase, and *rpoD*, encoding the  $\sigma^{70}$  subunit of RNA polymerase). It is unclear if *F. tularensis* cells lacking all three *rpsU* genes were viable.

The literature reflects that bS21 may regulate gene expression in other bacteria. A recent study of the *Flavobacterium johnsoniae* ribosome revealed that bS21 plays a role in sequestering the anti-Shine-Dalgarno sequence (43). This occlusion occurs through contacts with the C-terminal region of bS21 that are conserved across Bacteroidetes species and provided a rationale to explain why most Bacteroidetes mRNAs lack Shine-Dalgarno sequences. Notably, the mRNA encoding bS21 in *F. johnsoniae* encodes a perfect Shine-Dalgarno sequence, strongly suggesting that bS21 regulates its expression through translational autoregulation (43). *F. tularensis*, however, is a member of the Gammaproteobacteria, has bS21 homologs that exhibit significant differences from *F. johnsoniae* at the C-terminal region, and encodes mRNAs that commonly contain sequences similar to the consensus Shine-Dalgarno sequence. This suggests that in *F. tularensis*, bS21 exerts its effects on gene expression differently.

In other bacteria that encode it, loss of bS21 led to a variety of phenotypic changes. In *B. subtilis*, loss of bS21 results in biofilm and motility defects (44), and in *Listeria monocytogenes*, inactivation of bS21 is linked to stress resistance and altered transcript abundance (45, 46). *Staphylococcus aureus* lacking functional bS21 exhibits increased resistance to the antibiotics daptomycin and vancomycin (47–49). Both *Burkholderia pseudomallei* and *F. tularensis* encode multiple bS21 homologs and in both organisms, virulence screens using transposon mutagenesis have identified one homolog as

important for virulence (50, 51). Together, these findings suggested that bS21 may regulate gene expression in diverse bacterial species.

The idea that bS21 might modulate translation for a subset of mRNAs is further supported by the recent discovery that bS21 is encoded by thousands of sequenced bacteriophage genomes and is one of the most encoded phage ribosomal proteins (52, 53). Transcripts encoding bS21 have been detected in metatranscriptomic samples along with transcripts for late-stage replication proteins (54) and at least one phage-encoded bS21 can be incorporated into *E. coli* ribosomes (52). All of this raises the possibility that the incorporation of a viral bS21 into the host ribosome may co-opt the translation machinery in favor of viral proteins and replication.

Our work, together with these earlier findings, strongly suggested that the incorporation of bS21 into the ribosome could impact the translation of a subset of mRNAs. Considering that bS21 could easily be exchanged among ribosomes, this provided an excellent mechanism to quickly fine-tune the cellular proteome. While the molecular mechanism leading to the modulation of translation has yet to be identified, it is reasonable to speculate that bS21 impacted translation during initiation through specific interactions with the 5' untranslated regions of a specific set of mRNAs. These findings also supported the idea that changes in ribosome composition may impact translation and provided another source for bacterial control of gene expression.

## MATERIALS AND METHODS

**Bacterial strains and growth conditions.** Unless otherwise noted, bacterial strains were grown as indicated here. *Francisella tularensis* subsp. *holarctica* live vaccine strain (LVS) cells were grown in Mueller-Hinton broth (BD Difco) supplemented with 0.025% iron pyrophosphate, 0.1% glucose, and 2% Isovitalex (SMHB), shaking aerobically or on cystine heart agar plates with 1% hemoglobin (CHA-H) at 37°C. *Escherichia coli* XL1-Blue cells were grown in lysogeny broth (LB) shaking aerobically or on LB agar plates at 37°C. Kanamycin was used at concentrations of 5 µg/mL (*F. tularensis*) or 50 µg/mL (*E. coli*).

**Vector construction.** Complementation plasmids for each bS21 homolog were created from a plasmid derived from pFNLTp6 (55) and pKL42 (pF-PmrA-V). Specifically, the complementation plasmids produce bS21 homologs with a C-terminal VSV-G epitope under the control of the *F. tularensis* *groES* promoter. Each *rpsU* gene was amplified using a 5' primer specifying an EcoRI site and an ideal Shine-Dalgarno sequence (5'-AGGAGG-3') located six nucleotides upstream from the translation start site. The 3' primer did not include the native stop codon and included DNA specifying a NotI site. The fragment was cloned into EcoRI/NotI digested pKL42, such that the 3' end of each *rpsU* was in frame with codons specifying three alanines followed by the VSV-G epitope. The resulting plasmids were pKR6 pF-bS21-1-V, pKR7 pF-bS21-2-V, and pKR8 pF-bS21-3-V. The control plasmid pF was the original pFNLTp6 plasmid (containing the *groES* promoter but not any *rpsU* genes nor the VSV-G epitope).

The plasmid pEX18kan was modified to generate in-frame deletions of each *rpsU* gene as previously described (14). Flanking regions of ~600 bp from both sides of each *rpsU* gene were amplified by PCR. Primers amplifying the DNA adjacent to each *rpsU* gene included the first three or last three codons of the open reading frame and DNA specifying a NotI site, which also encodes an alanine linker (5'-GCCGCCGCT-3'). The two fragments were cloned into BamHI/KpnI-digested pEX18kan for each *rpsU* gene, respectively, yielding pKL122 pEXΔ*rpsU1*, pKR11 pEXΔ*rpsU2*, and pKR12 pEXΔ*rpsU3*; these plasmids were used to construct deletions via the allelic exchange as described below.

**Strain construction.** Deletion strains were constructed by the allelic exchange as previously (56). Briefly, competent cells were made by washing *F. tularensis* LVS cells in 10% sucrose and resuspending them in an equal volume of 10% sucrose to cells. At least 1 µg of allelic exchange plasmid was electroporated into 50 µL competent cells in 0.2 cm cuvettes with a 2.5 kV pulse. Cells were allowed to recover in 4 to 5 mL SMHB for 4 to 8 h at 37°C, shaking. Cells in which a single integration event occurred were selected on CHA-H plates with kanamycin. These cells were subsequently plated on CHA-H containing 10% sucrose and lacking NaCl, allowing for survival only of cells that had crossed out the nonhomologous portion of the vector, including *sacB* and kanamycin resistance gene. Colonies that were sucrose-resistant and kanamycin-sensitive were screened for deletions using PCR. Candidate strains were confirmed by amplification of genomic DNA outside the flanking regions on each side of the deletion and Sanger sequencing (Rhode Island Genomics and Sequencing Center). Plasmid pKL122 pEXΔ*rpsU1* was used to make LVS Δ*rpsU1*, plasmid pKR11 pEXΔ*rpsU2* was used to make LVS Δ*rpsU2*, and plasmid pKR12 pEXΔ*rpsU3* was used to make LVS Δ*rpsU3*.

Complementation plasmids were electroporated into LVS or LVS Δ*rpsU2* cells as described above and selected for on CHA-H plates with kanamycin.

**Immunoblotting.** Cells were collected from mid-log phase cultures (optical density at 600 nm (OD<sub>600</sub>) = 0.3 to 0.4) and resuspended in sample loading buffer (SLB: 1× NuPAGE LDS with 50 mM DTT) normalized to OD<sub>600</sub> and heated at 95°C for 10 min. Cell lysates and fractions were separated by SDS-PAGE on 4 to 12% Bis-Tris NuPAGE gels in MES or MOPS running buffer (Invitrogen) and transferred to PVDF with the Mini Blot Module transfer system (Invitrogen; 20 V for 1 h on ice) or the Criterion cell for midi gels (Bio-Rad; 60 V for 40 min on ice) with 1× NuPAGE transfer buffer and 10% methanol. Whole-cell lysates were analyzed for total protein with the Invitrogen No-Stain Protein labeling reagent and all



membranes were blocked with Odyssey blocking buffer diluted 1:5 in PBS overnight. For each antibody, the linear range of protein detection was determined by plotting sequential dilutions of one lysate from each strain as a standard curve to establish an appropriate volume of lysate to load. Membranes were probed with indicated monoclonal antibodies (BEI Resources, diluted 1:1000 in blocking buffer for all antibodies except anti-PdpB, which was diluted 1:250) or the VSV-G epitope (Sigma, diluted 1:2222). Proteins were detected using IRDye 800 CW donkey anti-mouse IgG or donkey anti-rabbit IgG (Li-Cor, diluted 1:10,000). Fluorescence was measured and quantified on the LiCor Odyssey CLx imager and software, and protein abundance was calculated relative to the total protein in each lane. Experiments were performed at least twice in biological triplicate and two to three technical replicates.

**RNA isolation and qRT-PCR.** Cells were collected from mid-log phase cultures ( $OD_{600} = 0.3$  to  $0.4$ ). Nucleic acids were isolated using the Direct-Zol RNA purification kit (Zymo Research) according to the manufacturer's protocol. Purified nucleic acids were treated with RQ1 DNase (Promega) for 1 h at  $37^{\circ}\text{C}$  and RNA was purified with the Direct-Zol RNA purification kit. cDNA was synthesized using Superscript III reverse transcriptase (Life Technologies) as previously described (14). qRT-PCR was performed using PowerUp SYBR Green Master Mix (Applied Biosystems) and a Roche LightCycler 480 (University of Rhode Island Genomics and Sequencing Center) essentially as described (14). Transcript abundances of *pdpA*, *pdpB*, *iglA*, and *pigR* were compared to three different control genes (*tul4*, *rpoA1*, and *bfr*) and since all results were similar, relative abundance was reported to *tul4*. Experiments comparing wild-type and *rpsU2* mutant cells were performed three times in biological triplicate. An experiment with cells lacking *PigR* was performed once.

**RNA-seq.** Approximately  $1.5\ \mu\text{g}$  of RNA isolated as above was sent to the Microbial Genome Sequencing Center (MiGS) for RNA-Seq analysis, in biological triplicate (LVS pF) or duplicate (LVS  $\Delta rpsU2$  pF, LVS  $\Delta rpsU2$  pF-b521-2-V). After using RiboZero Plus rRNA depletion, libraries were made using Illumina Stranded RNA library preparation and sequenced for a minimum of 12 million paired-end reads. Paired-end sequencing reads were mapped to the *F. tularensis* LVS genome (NCBI RefSeq accession number NC\_007880) using bowtie2 version 2.2.4. Reads that mapped to annotated genes were counted using HTSeq version 0.11.2, and analysis of differential gene expression was conducted using DESeq2 version 1.32.0. Reported genes had a 2-fold higher or lower abundance than the wild type, all with an adjusted *P* value of 0.05 or lower.

**70S ribosome purification.** 70S ribosomes were isolated using sucrose cushion centrifugation essentially as described (57). Briefly, wild-type *F. tularensis* cells were grown in 500 mL sMHB to mid-log phase ( $OD_{600} = 0.3$  to  $0.4$ ). Cells were chilled on ice for 20 min, centrifuged at  $11,000 \times g$  for 5 min at  $4^{\circ}\text{C}$ , then washed once with buffer  $\text{H}^{10}\text{M}^{10}\text{A}^{1000}$  (10 mM HEPES KOH pH 7.6, 10 mM  $\text{MgCl}_2$ , and 100 mM  $\text{NH}_4\text{Cl}$ ) to remove ribonucleases. The pellet was then washed twice with buffer  $\text{H}^{10}\text{M}^{10}\text{A}^{50}$  (10 mM HEPES KOH pH 7.6, 10 mM  $\text{MgCl}_2$ , and 50 mM  $\text{NH}_4\text{Cl}$ , with or without 5 mM  $\beta$ -mercaptoethanol [BME]), and resuspended in  $\sim 15\ \text{mL}$  of  $\text{H}^{10}\text{M}^{10}\text{A}^{50}$  with 20 U DNase I. Cells were lysed by passing through a French press three times at  $800\ \text{lb/in}^2$  and cell debris were removed by centrifugation at  $146,000 \times g$  for 15 min at  $4^{\circ}\text{C}$ . Supernatant was incubated with 0.5% Brij58 for 30 min and layered on top of  $\text{H}^{10}\text{M}^{10}\text{A}^{500} + 20\%$  sucrose (10 mM HEPES KOH pH 7.6, 10 mM  $\text{MgCl}_2$ , 500 mM  $\text{NH}_4\text{Cl}$ , 20% sucrose, with or without 5 mM BME). Ribosomes were pelleted by ultracentrifugation in a 70 Ti rotor for 4 h at  $146,000 \times g$  at  $4^{\circ}\text{C}$ . The pellet was washed twice with  $\text{H}^{10}\text{M}^{10}\text{A}^{50}$  and gently resuspended in  $\text{H}^{10}\text{M}^{10}\text{A}^{50}$ . This suspension was then layered onto another sucrose cushion ( $\text{H}^{10}\text{M}^{10}\text{A}^{50}$  with 40% sucrose) and centrifuged for 14 h at  $146,000 \times g$  at  $4^{\circ}\text{C}$  to further purify the ribosomes. Purified 70S ribosomes were gently resuspended in  $\sim 250\ \mu\text{L}$  of  $\text{H}^{10}\text{M}^{10}\text{A}^{50}$  and stored at  $-80^{\circ}\text{C}$ .

**LC-MS/MS of purified LVS ribosomes.** 70S ribosomes from wild-type LVS cells were prepared as described above. Samples were either purified via gel stacking before mass spectrometry analysis or maintained in  $\text{H}^{10}\text{M}^{10}\text{A}^{50}$  and delivered to the Northwestern Proteomics Core. The proteins were in-gel digested or in-solution digested and liquid chromatography-tandem mass spectrometry (LC-MS/MS) analysis was completed based on internal protocols, matching peptides to the *F. tularensis* LVS proteome (NC\_007880).

**DIA mass spectrometry.** Cells were collected from mid-log phase cultures ( $OD_{600} = 0.3$  to  $0.4$ ) and resuspended in Buffer 1 (20 mM HEPES pH 7.9, 50 mM KCl, 0.5 mM DTT) with protease inhibitor tablets (Complete Mini, EDTA-free, Roche). Cells were lysed by sonication and protein concentration was determined using a BCA protein assay (Pierce). Lysates with concentrations between 620 and  $862\ \mu\text{g/mL}$  were used by the University of Arkansas for Medical Sciences (UAMS) Proteomics Core for analysis. Protein extraction and protease digestion were completed according to UAMS internal protocols. Data-independent acquisition (DIA) was completed with the Orbitrap Exploris 480 mass spectrometer.

**Polysome purification and sucrose gradient sedimentation.** Polysomes were isolated essentially as described (58). *F. tularensis* cells were grown until early log ( $OD_{600}$  0.2 to 0.25). Liquid cultures were rapidly filtered through  $0.2\ \mu\text{m}$  nitrocellulose membranes and transferred to a conical tube filled with liquid nitrogen. Cells were lysed by bead-beating with  $650\ \mu\text{L}$  flash frozen lysis buffer (25 mM HEPES pH 7.6, 100 mM  $\text{NH}_4\text{Cl}$ , 10 mM  $\text{MgCl}_2$ , 0.4% Triton X-100, 0.1% NP-40, 100 U/mL Rnase-free Dnase) using the TissueLyser II (Qiagen) five times (15 Hz, 3 min). Cell debris was pelleted and the polysome-containing lysates were stored at  $-80^{\circ}\text{C}$ .

Sucrose gradients were prepared using 10% and 55% sucrose solutions in 25 mM HEPES pH 7.6, 100 mM  $\text{NH}_4\text{Cl}$ , 10 mM  $\text{MgCl}_2$  with the BioComp Instruments 153 Gradient Station (BioComp). Cell lysates were layered onto gradients and centrifuged with the Beckman-Coulter SW40 Ti rotor at 40,000 rpm for 2.5 h at  $4^{\circ}\text{C}$ . Gradients were fractionated using the Triax full spectrum flow cell and fractionator (BioComp;  $0.2\ \text{mm/s}$ , 28 fractions), and A260 was measured every second. Collected fractions



were stored at  $-80^{\circ}\text{C}$ . 20  $\mu\text{L}$  of each fraction was combined with 10  $\mu\text{L}$  of sample loading buffer ( $3\times$  NuPAGE LDS with 50 mM DTT) and immunoblotted as described above.

**Intramacrophage replication assays.** Intramacrophage growth assays were performed as previously described (56). Briefly, approximately  $2.5 \times 10^4$  cells of murine macrophage-like J774A.1 cells were incubated at  $37^{\circ}\text{C}$  in 5%  $\text{CO}_2$  overnight in 96-well plates in DMEM (Invitrogen) supplemented with 10% fetal bovine serum (Gemini Bio-Products; DMEM-F). Macrophage cells were infected with LVS and indicated derivative strains at an MOI of approximately 5 to 10. After 2 h, cells were washed twice with PBS, and the medium was replaced with DMEM-F containing 10  $\mu\text{g}/\text{mL}$  gentamicin. After 2 h or 24 h of infection, macrophages were lysed for 30 min in 1% saponin in PBS and plated for enumeration.

**Antibiotic chase experiment.** Indicated *F. tularensis* LVS cells were grown to mid-log phase in liquid culture ( $\text{OD}_{600} = 0.3$  to  $0.4$ ). Spectinomycin was added to a final concentration of 200  $\mu\text{g}/\text{mL}$ . Cells were collected at the indicated time points after antibiotic addition and resuspended in a sample loading buffer normalized to  $\text{OD}_{600}$  at  $t = 0$ . Immunoblotting was conducted as described above and analysis was conducted using a one-phase decay equation on Prism 9 (GraphPad). Data represent two experiments in biological triplicate.

**Data availability.** RNA-Seq reads are available in the National Center for Biotechnology Information Gene Expression Omnibus (NCBI GEO) under accession number GSE210766.

## SUPPLEMENTAL MATERIAL

Supplemental material is available online only.

**SUPPLEMENTAL FILE 1**, PDF file, 4.8 MB.

**SUPPLEMENTAL FILE 2**, XLSX file, 0.03 MB.

**SUPPLEMENTAL FILE 3**, XLSX file, 0.3 MB.

**SUPPLEMENTAL FILE 4**, XLSX file, 0.3 MB.

**SUPPLEMENTAL FILE 5**, XLSX file, 0.01 MB.

## ACKNOWLEDGMENTS

For helpful comments on the manuscript, we thank Simon L. Dove, Steven T. Gregory, and Matthew M. Ramsey. For use of shared equipment, we thank Gregory, Jodi L. Camberg, and Niall G. Howlett. We thank the other members of the Ramsey laboratory. We also thank Janet Atoyán and the URI Genomics and Sequencing Center (now Rhode Island INBRE Molecular Informatics Core).

This work was funded by an NIGMS CARTD-COBRE Pilot Project Award (P20GM121344-KMR), an NIGMS/RI-INBRE Early Career Development Award (P20GM103430-KMR), and a Rhode Island Foundation Medical Research Grant (2798\_20190602-KMR). This work was supported by the USDA National Institute of Food and Agriculture, Hatch Formula project accession number 1017848. This material was based upon work conducted at a Rhode Island NSF EPSCoR research facility, the Genomics and Sequencing Center, supported in part by the National Science Foundation EPSCoR Cooperative Agreements 0554548, EPS-1004057, and OIA-1655221. The research was made possible using equipment and services available through the Rhode Island Institutional Development Award (IDeA) Network of Biomedical Research Excellence from the National Institute of General Medical Sciences of the National Institutes of Health under grant number P20GM103430 through the Centralized Research Core facility and the Molecular Informatics Core (RRID:SCR\_017685). LC-MS/MS proteomics was performed by the Northwestern Proteomics Core Facility, supported by NCI CCSG P30 CA060553, instrumentation award (S10OD025194), and the National Resource for Translational and Developmental Proteomics supported by P41 GM108569. DIA proteomics was performed by IDeA National Resource for Quantitative Proteomics, supported by NIGMS R24GM137786. Antibodies for the following *Francisella tularensis* proteins were obtained through BEI Resources, NIAID, NIH: PdpB, IgIA, IgIB, IgIC, and IgID.

AQ: C We declare no conflict of interest.

## REFERENCES

1. Hershey JWB, Sonenberg N, Mathews MB. 2012. Principles of translational control: an overview. *Csh Perspect Biol* 4:a011528–a011528. <https://doi.org/10.1101/cshperspect.a011528>.
2. Duval M, Simonetti A, Caldelari I, Marzi S. 2015. Multiple ways to regulate translation initiation in bacteria: mechanisms, regulatory circuits, dynamics. *Biochimie* 114:18–29. <https://doi.org/10.1016/j.biochi.2015.03.007>.

3. Byrgazov K, Vesper O, Moll I. 2013. Ribosome heterogeneity: another level of complexity in bacterial translation regulation. *Curr Opin Microbiol* 16: 133–139. <https://doi.org/10.1016/j.mib.2013.01.009>.
4. Xue S, Barna M. 2012. Specialized ribosomes: a new frontier in gene regulation and organismal biology. *Nat Rev Mol Cell Biol* 13:355–369. <https://doi.org/10.1038/nrm3359>.
5. Kurylo CM, Parks MM, Juette MF, Zinshteyn B, Altman RB, Thibado JK, Vincent CT, Blanchard SC. 2018. Endogenous rRNA sequence variation can regulate stress response gene expression and phenotype. *Cell Rep* 25:236–248.e6. <https://doi.org/10.1016/j.celrep.2018.08.093>.
6. Song W, Joo M, Yeom J-H, Shin E, Lee M, Choi H-K, Hwang J, Kim Y-I, Seo R, Lee JE, Moore CJ, Kim Y-H, Eyun S-I, Hahn Y, Bae J, Lee K. 2019. Divergent rRNAs as regulators of gene expression at the ribosome level. *Nat Microbiol* 4:515–526. <https://doi.org/10.1038/s41564-018-0341-1>.
7. Chen Y-X, Xu Z, Ge X, Hong J-Y, Sanyal S, Lu ZJ, Javid B. 2020. Selective translation by alternative bacterial ribosomes. *Proc Natl Acad Sci U S A* 117:19487–19496. <https://doi.org/10.1073/pnas.2009607117>.
8. Sjöstedt A. 2007. Tularemia: history, epidemiology, pathogen physiology, and clinical manifestations. *Ann N Y Acad Sci* 1105:1–29. <https://doi.org/10.1196/annals.1409.009>.
9. Barker JR, Chong A, Wehrly TD, Yu J-J, Rodriguez SA, Liu J, Celli J, Arulanandam BP, Klose KE. 2009. The *Francisella tularensis* pathogenicity island encodes a secretion system that is required for phagosome escape and virulence. *Mol Microbiol* 74:1459–1470. <https://doi.org/10.1111/j.1365-2958.2009.06947.x>.
10. Bröms JE, Meyer L, Sun K, Lavander M, Sjöstedt A. 2012. Unique substrates secreted by the type VI secretion system of *Francisella tularensis* during intramacrophage infection. *PLoS One* 7:e50473. <https://doi.org/10.1371/journal.pone.0050473>.
11. Eshraghi A, Kim J, Walls AC, Ledvina HE, Miller CN, Ramsey KM, Whitney JC, Radey MC, Peterson SB, Ruhland BR, Tran BQ, Goo YA, Goodlett DR, Dove SL, Celli J, Veesler D, Mougous JD. 2016. Secreted effectors encoded within and outside of the *Francisella* pathogenicity island promote intramacrophage growth. *Cell Host Microbe* 20:573–583. <https://doi.org/10.1016/j.chom.2016.10.008>.
12. Ledvina HE, Kelly KA, Eshraghi A, Plemel RL, Peterson SB, Lee B, Steele S, Adler M, Kawula TH, Merz AJ, Skerrett SJ, Celli J, Mougous JD. 2018. A phosphatidylinositol 3-kinase effector alters phagosomal maturation to promote intracellular growth of *Francisella*. *Cell Host Microbe* 24: 285–295.e8. <https://doi.org/10.1016/j.chom.2018.07.003>.
13. Lauriano CM, Barker JR, Yoon S-S, Nano FE, Arulanandam BP, Hassett DJ, Klose KE. 2004. MglA regulates transcription of virulence factors necessary for *Francisella tularensis* intramacrophage and intramacrophage survival. *Proc Natl Acad Sci U S A* 101:4246–4249. <https://doi.org/10.1073/pnas.0307690101>.
14. Charity JC, Costante-Hamm MM, Balon EL, Boyd DH, Rubin EJ, Dove SL. 2007. Twin RNA polymerase-associated proteins control virulence gene expression in *Francisella tularensis*. *PLoS Pathog* 3:e84. <https://doi.org/10.1371/journal.ppat.0030084>.
15. Charity JC, Blalock LT, Costante-Hamm MM, Kasper DL, Dove SL. 2009. Small molecule control of virulence gene expression in *Francisella tularensis*. *PLoS Pathog* 5:e1000641. <https://doi.org/10.1371/journal.ppat.1000641>.
16. Brotcke A, Monack DM. 2008. Identification of *fevR*, a novel regulator of virulence gene expression in *Francisella novicida*. *Infect Immun* 76: 3473–3480. <https://doi.org/10.1128/IAI.00430-08>.
17. Rohlfing AE, Dove SL. 2014. Coordinate control of virulence gene expression in *Francisella tularensis* involves direct interaction between key regulators. *J Bacteriol* 196:3516–3526. <https://doi.org/10.1128/JB.01700-14>.
18. Ramsey KM, Osborne ML, Vvedenskaya IO, Su C, Nickels BE, Dove SL. 2015. Ubiquitous promoter-localization of essential virulence regulators in *Francisella tularensis*. *PLoS Pathog* 11:e1004793. <https://doi.org/10.1371/journal.ppat.1004793>.
19. Cuthbert BJ, Ross W, Rohlfing AE, Dove SL, Gourse RL, Brennan RG, Schumacher MA. 2017. Dissection of the molecular circuitry controlling virulence in *Francisella tularensis*. *Genes Dev* 31:1549–1560. <https://doi.org/10.1101/gad.303701.117>.
20. Travis BA, Ramsey KM, Prezioso SM, Tallo T, Wandzilak JM, Hsu A, Borgnia M, Bartesaghi A, Dove SL, Brennan RG, Schumacher MA. 2021. Structural basis for virulence activation of *Francisella tularensis*. *Mol Cell* 81:139–152.e10. <https://doi.org/10.1016/j.molcel.2020.10.035>.
21. Duin JV, Wijnands R. 1981. The function of ribosomal protein S21 in protein synthesis. *Eur J Biochem* 118:615–619. <https://doi.org/10.1111/j.1432-1033.1981.tb05563.x>.
22. Chang C, Craven GR. 1977. Identification of several proteins involved in the messenger RNA binding site of the 30 S ribosome by inactivation with 2-methoxy-5-nitropropene. *J Mol Biol* 117:401–418. [https://doi.org/10.1016/0022-2836\(77\)90135-8](https://doi.org/10.1016/0022-2836(77)90135-8).
23. Berk V, Zhang W, Pai RD, Cate JHD, Cate JHD. 2006. Structural basis for mRNA and tRNA positioning on the ribosome. *Proc Natl Acad Sci U S A* 103:15830–15834. <https://doi.org/10.1073/pnas.0607541103>.
24. Watson ZL, Ward FR, Méheust R, Ad O, Schepartz A, Banfield JF, Cate JH. 2020. Structure of the bacterial ribosome at 2 Å resolution. *Elife* 9:e60482. <https://doi.org/10.7554/eLife.60482>.
25. Mizushima S, Nomura M. 1970. Assembly mapping of 30S ribosomal proteins from *E. coli*. *Nature* 226:1214–1218. <https://doi.org/10.1038/2261214a0>.
26. Robertson WR, Dowsett SJ, Hardy SJS. 1977. Exchange of ribosomal proteins among the ribosomes of *Escherichia coli*. *Mol Gen Genet* 157: 205–214. <https://doi.org/10.1007/BF00267399>.
27. Lupski JR, Godson GN. 1984. The *rpsU-dnaG-rpoD* macromolecular synthesis operon of *E. coli*. *Cell* 39:251–252. [https://doi.org/10.1016/0092-8674\(84\)90001-1](https://doi.org/10.1016/0092-8674(84)90001-1).
28. Deniziak M, Sauter C, Becker HD, Paulus CA, Giegé R, Kern D. 2007. Deino-coccus glutaminyl-tRNA synthetase is a chimera between proteins from an ancient and the modern pathways of aminoacyl-tRNA formation. *Nucleic Acids Res* 35:1421–1431. <https://doi.org/10.1093/nar/gkl1164>.
29. Searle BC, Swearingen KE, Barnes CA, Schmidt T, Gessulat S, Küster B, Wilhelm M. 2020. Generating high quality libraries for DIA MS with empirically corrected peptide predictions. *Nat Commun* 11:1548. <https://doi.org/10.1038/s41467-020-15346-1>.
30. Takata R. 1978. Genetic studies of the ribosomal proteins in *Escherichia coli* XI. *Mol Gen Genet* 160:151–155. <https://doi.org/10.1007/BF00267476>.
31. Nomura M, Gourse R, Baughman G. 1984. Regulation of the synthesis of ribosomes and ribosomal components. *Annu Rev Biochem* 53:75–117. <https://doi.org/10.1146/annurev.bi.53.070184.000451>.
32. Nano FE, Zhang N, Cowley SC, Klose KE, Cheung KKM, Roberts MJ, Ludu JS, Letendre GW, Meierovics AI, Stephens G, Elkins KL. 2004. A *Francisella tularensis* pathogenicity island required for intramacrophage growth. *J Bacteriol* 186:6430–6436. <https://doi.org/10.1128/JB.186.19.6430-6436.2004>.
33. Larsson P, Oyston PCF, Chain P, Chu MC, Duffield M, Fuxelius H-H, Garcia E, Hålltorp G, Johansson D, Isherwood KE, Karp PD, Larsson E, Liu Y, Michell S, Prior R, Prior R, Malfatti S, Sjöstedt A, Svensson K, Thompson N, Vergez L, Wagg JK, Wren BW, Lindler LE, Andersson SGE, Forsman M, Titball RW. 2005. The complete genome sequence of *Francisella tularensis*, the causative agent of tularemia. *Nat Genet* 37:153–159. <https://doi.org/10.1038/ng1499>.
34. Nano FE, Schmek C. 2007. The *Francisella* pathogenicity island. *Ann N Y Acad Sci* 1105:122–137. <https://doi.org/10.1196/annals.1409.000>.
35. Brotcke A, Weiss DS, Kim CC, Chain P, Malfatti S, Garcia E, Monack DM. 2006. Identification of MglA-regulated genes reveals novel virulence factors in *Francisella tularensis*. *Infect Immun* 74:6642–6655. <https://doi.org/10.1128/IAI.01250-06>.
36. Vargas-Blanco DA, Shell SS. 2020. Regulation of mRNA stability during bacterial stress responses. *Front Microbiol* 11:2111. <https://doi.org/10.3389/fmicb.2020.02111>.
37. Yutin N, Puigbo P, Koonin EV, Wolf YI. 2012. Phylogenomics of prokaryotic ribosomal proteins. *PLoS One* 7:e36972. <https://doi.org/10.1371/journal.pone.0036972>.
38. Galperin MY, Wolf YI, Garushyants SK, Alvarez RV, Koonin EV. 2021. Nonessential ribosomal proteins in bacteria and archaea identified using clusters of orthologous genes. *J Bacteriol* 203:e00058-21. <https://doi.org/10.1128/JB.00058-21>.
39. Bubunenkov M, Baker T, Court DL. 2007. Essentiality of ribosomal and transcription antitermination proteins analyzed by systematic gene replacement in *Escherichia coli*. *J Bacteriol* 189:2844–2853. <https://doi.org/10.1128/JB.01713-06>.
40. Yamamoto N, Nakahigashi K, Nakamichi T, Yoshino M, Takai Y, Touda Y, Furubayashi A, Kinjo S, Dose H, Hasegawa M, Datsenko KA, Nakayashiki T, Tomita M, Wanner BL, Mori H. 2009. Update on the Keio collection of *Escherichia coli* single-gene deletion mutants. *Mol Syst Biol* 5:335. <https://doi.org/10.1038/msb.2009.92>.
41. Goodall ECA, Robinson A, Johnston IG, Jabbari S, Turner KA, Cunningham AF, Lund PA, Cole JA, Henderson IR. 2018. The essential genome of *Escherichia coli* K-12. *mBio* 9:e02096-17. <https://doi.org/10.1128/mBio.02096-17>.
42. Ramsey KM, Ledvina HE, Tresko TM, Wandzilak JM, Tower CA, Tallo T, Schramm CE, Peterson SB, Skerrett SJ, Mougous JD, Dove SL. 2020. Tn-seq reveals hidden complexity in the utilization of host-derived glutathione

- in *Francisella tularensis*. PLoS Pathog 16:e1008566. <https://doi.org/10.1371/journal.ppat.1008566>.
43. Jha V, Roy B, Jahagirdar D, McNutt ZA, Shatoff EA, Boleratz BL, Watkins DE, Bundschuh R, Basu K, Ortega J, Fredrick K. 2021. Structural basis of sequestration of the anti-Shine-Dalgarno sequence in the Bacteroidetes ribosome. Nucleic Acids Res 49:547–567. <https://doi.org/10.1093/nar/gkaa1195>.
  44. Takada H, Morita M, Shiwa Y, Sugimoto R, Suzuki S, Kawamura F, Yoshikawa H. 2014. Cell motility and biofilm formation in *Bacillus subtilis* are affected by the ribosomal proteins, S11 and S21. Biosci Biotechnol Biochem 78:898–907. <https://doi.org/10.1080/09168451.2014.915729>.
  45. Metselaar KI, den Besten HMW, Boekhorst J, van Hijum SAFT, Zwietering MH, Abee T. 2015. Diversity of acid stress resistant variants of *Listeria monocytogenes* and the potential role of ribosomal protein S21 encoded by *rpsU*. Front Microbiol 6:422.
  46. Metselaar KI, Abee T, Zwietering MH, den Besten HMW. 2016. Modeling and validation of the ecological behavior of wild-type *Listeria monocytogenes* and stress-resistant variants. Appl Environ Microbiol 82:5389–5401. <https://doi.org/10.1128/AEM.00442-16>.
  47. Basco MDS, Kothari A, McKinzie PB, Revollo JR, Agnihothram S, Azevedo MP, Saccente M, Hart ME. 2019. Reduced vancomycin susceptibility and increased macrophage survival in *Staphylococcus aureus* strains sequentially isolated from a bacteraemic patient during a short course of antibiotic therapy. J Med Microbiol 68:848–859. <https://doi.org/10.1099/jmm.0.000988>.
  48. Blake KL, O'Neill AJ. 2013. Transposon library screening for identification of genetic loci participating in intrinsic susceptibility and acquired resistance to antistaphylococcal agents. J Antimicrob Chemother 68:12–16. <https://doi.org/10.1093/jac/dks373>.
  49. Friedman L, Alder JD, Silverman JA. 2006. Genetic changes that correlate with reduced susceptibility to daptomycin in *Staphylococcus aureus*. Antimicrob Agents Chemother 50:2137–2145. <https://doi.org/10.1128/AAC.00039-06>.
  50. Gutierrez MG, Yoder-Himes DR, Warawa JM. 2015. Comprehensive identification of virulence factors required for respiratory melioidosis using Tn-seq mutagenesis. Front Cell Infect Microbiol 5:78. <https://doi.org/10.3389/fcimb.2015.00078>.
  51. Su J, Yang J, Zhao D, Kawula TH, Banas JA, Zhang J-R. 2007. Genome-wide identification of *Francisella tularensis* virulence determinants. Infect Immun 75:3089–3101. <https://doi.org/10.1128/IAI.01865-06>.
  52. Mizuno CM, Guyomar C, Roux S, Lavigne R, Rodriguez-Valera F, Sullivan MB, Gillet R, Forterre P, Krupovic M. 2019. Numerous cultivated and uncultivated viruses encode ribosomal proteins. Nat Commun 10:752. <https://doi.org/10.1038/s41467-019-08672-6>.
  53. Al-Shayeb B, Sachdeva R, Chen L-X, Ward F, Munk P, Devoto A, Castelle CJ, Olm MR, Bouma-Gregson K, Amano Y, He C, Méheust R, Brooks B, Thomas A, Lavy A, Matheus-Carnevali P, Sun C, Goltsman DSA, Borton MA, Sharrar A, Jaffe AL, Nelson TC, Kantor R, Keren R, Lane KR, Farag IF, Lei S, Finstad K, Amundson R, Anantharaman K, Zhou J, Probst AJ, Power ME, Tringe SG, Li W-J, Wrighton K, Harrison S, Morowitz M, Relman DA, Doudna JA, Lehours A-C, Warren L, Cate JHD, Santini JM, Banfield JF. 2020. Clades of huge phages from across Earth's ecosystems. Nature 578:425–431. <https://doi.org/10.1038/s41586-020-2007-4>.
  54. Chen L-X, Jaffe AL, Borges AL, Penev PI, Nelson TC, Warren LA, Banfield JF. 2022. Phage-encoded ribosomal protein S21 expression is linked to late-stage phage replication. ISME Commun 2:31. <https://doi.org/10.1038/s43705-022-00111-w>.
  55. Maier TM, Havig A, Casey M, Nano FE, Frank DW, Zahrt TC. 2004. Construction and characterization of a highly efficient *Francisella* shuttle plasmid. Appl Environ Microbiol 70:7511–7519. <https://doi.org/10.1128/AEM.70.12.7511-7519.2004>.
  56. Ramsey KM, Dove SL. 2016. A response regulator promotes *Francisella tularensis* intramacrophage growth by repressing an anti-virulence factor. Mol Microbiol 101:688–700. <https://doi.org/10.1111/mmi.13418>.
  57. Skeggs PA, Thompson J, Cundliffe E. 1985. Methylation of 16S ribosomal RNA and resistance to aminoglycoside antibiotics in clones of *Streptomyces lividans* carrying DNA from *Streptomyces tenjimariensis*. Mol Gen Genet 200:415–421. <https://doi.org/10.1007/BF00425725>.
  58. Johnson GE, Li G-W. 2018. Genome-wide quantitation of protein synthesis rates in bacteria. Methods Enzymol 612:225–249. <https://doi.org/10.1016/bs.mie.2018.08.031>.

## AUTHOR QUERIES

**Below are queries from the copy editor indicating specific areas of concern. Please respond in-line in the main text above, either by marking a change or indicating “ok.”**

1

AQau—Please make certain that all authors’ names are spelled correctly, and confirm the givennames and surnames are identified properly by the colors (this is important for how the names are indexed).

■ = Given-Name, ■ = Surname

AQabbr—Please check any added introductions of abbreviations and correct them if necessary.

AQdata—ASM policy requires that data be available to the public upon online posting of the article, so please verify all links to sequence records, if present, and make sure that each number retrieves the full record of the data. If a new accession number is not linked in the proof or a link is broken, provide the correct URL for the record. If the accession numbers for new data are not publicly accessible by the proof stage, publication of your article may be delayed; please contact the ASM production staff immediately with the expected release date.

AQfund— The table below includes funding information that you provided on the submission form when you submitted the manuscript. This funding information will not appear in the article, but it will be provided to CrossRef and made publicly available. Please check it carefully for accuracy and mark any necessary corrections. If you would like statements acknowledging financial support to be published in the article itself, please make sure that they appear in the Acknowledgments section. Statements in Acknowledgments will have no bearing on funding data deposited with CrossRef and vice versa.

Funder	Grant(s)	Author(s)	Funder ID
HHS   NIH   National Institute of General Medical Sciences (NIGMS)	P20GM121344, P20GM103430	Kathryn M. Ramsey	<a href="https://doi.org/10.13039/1000000057">https://doi.org/10.13039/1000000057</a>
Rhode Island Foundation	2798_20190602	Kathryn M. Ramsey	<a href="https://doi.org/10.13039/100014082">https://doi.org/10.13039/100014082</a>
U.S. Department of Agriculture (USDA)	1017848	Kathryn M. Ramsey	<a href="https://doi.org/10.13039/100000199">https://doi.org/10.13039/100000199</a>

AQA—The conflict of interest statement in this footnote is the statement of record and will appear in PubMed. Please confirm or correct the wording.

AQB—Kindly check if all supplemental material has been referenced correctly.

## AUTHOR QUERIES

**Below are queries from the copy editor indicating specific areas of concern. Please respond in-line in the main text above, either by marking a change or indicating “ok.”**

2

AQC—Please provide any conflict of interest.

---

PROOF